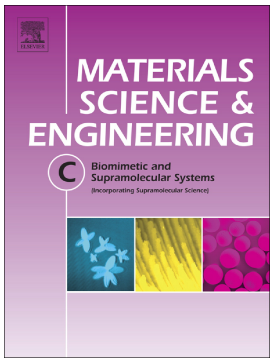

Live-cell biosensor for assessment of adhesion qualities of biomaterials

Svetlana I. Ivanova, Stoyan Chakarov, Albena Momchilova, Roumen Pankov

PII: S0928-4931(17)30953-0
DOI: doi: 10.1016/j.msec.2017.04.071
Reference: MSC 7894

To appear in: *Materials Science & Engineering C*

Received date: 12 March 2017
Accepted date: 13 April 2017

Please cite this article as: Svetlana I. Ivanova, Stoyan Chakarov, Albena Momchilova, Roumen Pankov , Live-cell biosensor for assessment of adhesion qualities of biomaterials. The address for the corresponding author was captured as affiliation for all authors. Please check if appropriate. Msc(2017), doi: 10.1016/j.msec.2017.04.071

Live-Cell Biosensor for Assessment of Adhesion Qualities of Biomaterials

Svetlana I. Ivanova[a], Stoyan Chakarov[b], Albena Momchilova[c], Roumen Pankov[a]*

[a] Department of Cytology, Histology and Embryology, Faculty of Biology, Sofia University "St. Kliment Ohridski", Sofia, Bulgaria
[b] Department of Biochemistry, Faculty of Biology, Sofia University "St. Kliment Ohridski", Sofia, Bulgaria
[c] Institute of Biophysics and Biomedical Engineering, Bulgarian Academy of Sciences, 1 Acad, Georgi Bonchev Str., block 21, 1113 Sofia, Bulgaria
* Corresponding author at: Department of Cytology, Histology and Embryology, Faculty of Biology, Sofia University "St. Kliment Ohridski", 8 Dragan Tzankov Blvd., 1164 Sofia, Bulgaria, E-mail address: rpankov@biofac.uni-sofia.bg (R. Pankov)

Abstract

The present study describes a live-cell biosensor, suitable for general evaluation of adhesion qualities of different substrates. It is based on NIH/3T3 fibroblast cell line stably expressing fusion fluorescently tagged proteins mCherry-vinculin and GFP-tensin as quantifiable markers for assessment not only of focal but also of fibrillar contacts. Four measurable parameters - spreading, polarization and development of focal and fibrillar adhesions were used to standardize the adhesion of biosensor cells after plating on five substrates of natural origin - fibronectin, vitronectin, laminin-111, laminin-521 and collagen type I. The obtained set of values (adhesion quality map) were utilized to describe the default biosensor behaviour and as a standard for evaluation of surface biocompatibility of materials with unknown adhesive properties. To demonstrate the applicability of the biosensor we studied two PDMS-based artificial materials. The results demonstrated the superior adhesive properties of the poly(acrylic acid)-containing polymer (PDMS-PAA) over that of poly(vinyl pyrrolidone) copolymer (PDMS-PVP), and pointed out the formation of focal adhesions as a parameter for possible further improvements.

Keywords: live-cell biosensor, biocompatibility, biomaterials, PDMS, cell adhesions.

1. Introduction

The successful implantation of biomaterials unconditionally requires interaction with cells which is exhibited through formation of adhesive contacts. These contacts ensure the correct functioning of key signal-transduction pathways which guide cell physiology and metabolism. The type, morphological characteristics and area of adhesions as well as cell spreading and polarization may refer as cell's functional status criteria [1], hence, as a tool for evaluation of the surface properties of adhesive materials [2].

Adhesion is a complex multi-stage process that initiates with attachment and spreading as the suspended cells lose their spherical shape and become flat and polarized. The major driving mechanism of spreading is the polymerization of actin filaments which push the membrane forward. At these very early stages of contact with the microenvironment cells form lamelipodia and "probe" the substrate in search of favourable adhesion sites. The first adhesion contacts to be formed are the focal complexes which in the appropriate ligand surroundings and substrate stiffness rapidly mature into the more stable focal adhesions (FA) [3]. Once the cell has established a stable attachment the onset of polarization begins and fibrillar adhesions (FbA) start to form. FbA originate from FA that serve as anchoring points from which activated $\alpha_5\beta_1$ integrins translocate centripetally along the actin stress fibres [4]. Simultaneously, the polymerization of fibronectin and the formation of fibronectin fibrils onto the cell surface are initiated and own extracellular matrix (ECM) deposition begins [5]. The number and total area of focal adhesions indicate the strength of cell attachment and portray a general depiction of cell physiological state [6, 7]. Fibrillar contact formation, on the other hand, testifies the initiation of fibrillogenesis and matrix formation [4]; processes to appear with cell remodelling of microenvironment in a tendency of lasting residence.

Numerous integrin receptors, anchoring cytoskeletal and adapter molecules are located into FA including vinculin and tensin [8, 9]. Unlike FA, FbA are composed mainly of actin fibrils crossed by the actin-binding protein tensin [4, 10]. Since no detectable vinculin molecules are localized in FbA [11, 12], the registry of co-localized vinculin and tensin can be used for identification of FA, while the presence only of tensin, without vinculin, gives evidence of FbA structures. Thus, based on these intrinsic localization differences, a combination of fluorescently tagged vinculin and tensin, expressed concurrently, can be employed for simultaneous detection of FA and FbA within the same cell. Taken together, these data led us to hypothesize that surface biocompatibility of new materials can be assessed in a consistent way by biosensor, representing live cell, designed to provide quantifiable information for cell adhesion contacts and cell morphology, manifested as spreading and polarization.

2. Materials and Methods

2.1. Materials and Instruments

NIH/3T3 cell line was purchased from ATCC. Anti-vinculin antibody (VIN-11-5), fibronectin and laminin-111 were purchased from Sigma; anti-GFP antibody (7.1/13.1) was from Roche; G418 was from Calbiochem; puromycin was from AppliChem; vitronectin was from Gibco; laminin-521 was from Biolamina; collagen type I was from Invitrogen. Electroporation was performed with a Gene Pulser Xcell (Bio-Rad) and microscope analyses with Axiovert 200M microscope equipped with an AxioCam MRm camera from Carl Zeiss.

2.2. Cell culture, transfection and immunoblotting

NIH/3T3 cells were cultured in high glucose DMEM supplemented with 10% bovine calf serum, 100 U/ml penicillin and 100 μg/ml streptomycin at 37ºC in a humidified 5% CO_2/95% air atmosphere.

Cells were co-transfected with pRKGFP-tensin and pmCherry-vinculin vectors in equimolar concentrations and pHA262 Puro A (encoding puromycin resistance gene) in five fold less quantity. Electroporation was carried out in 10 mM Na-phosphate, 1 mM $MgCl_2$ and 250 mM sucrose (pH 7.4) in a cuvette with 0.2 cm electrode gap by ten square wave pulses at a frequency of 1 Hz, duration of 5 ms each at 0.6 kV/cm.

Stably expressing cell lines were selected using G418 (a resistance gene encoded in the pmCherry vector) at a final concentration of 1000 μg/ml and 2 μg/ml puromycin.

Immunoblotting was performed as described [4].

2.3. Coating procedures and adhesion assays

All adhesion tests were performed on 12 mm coverslips coated with different substrates. Fibronectin and vitronectin were freshly diluted in PBS prior to coating; laminin-111 and laminin-521 were diluted in DMEM and collagen was prepared in 0.02 M acetic acid. Coating was carried out for 1 h at 37ºC followed by blocking with 1% heat denatured BSA for 1 h at 37ºC. For assessment of adhesive contacts cells ($0.5\text{-}1x10^4/cm^2$) were cultured overnight and fixed; for examination of spreading and polarization they were cultured for one and three hours, fixed and stained with Coomassie Brilliant Blue R-250.

Poly(dimethylsiloxane-b-acrylic acid) (PDMS-PAA) was 8.0-2.7 kDa and poly(dimethylsiloxane-b-vinyl pyrrolidone) (PDMS-PVP) was at a ratio of 80 wt.%:20 wt.%. PDMS solutions were spread on a 12 mm round coverslip, left overnight to dry at room temperature, rinsed in PBS, once in 70% ethanol and air dried. Before plating, substrates were washed in serum-free DMEM/25 mM HEPES.

2.4. Microscopy

Cells were fixed in 4% paraformaldehyde/10% sucrose (pH 7.2-7.4) for 20 min and mounted in Mowiol (0.6% Mowiol 4-88, 1.5% glycerol, 96 mM Tris-Cl pH 8.5, 2.5% DABCO and 0.1 μg/ml DAPI). For analysis of spreading and polarization, fixed cells were stained in 0.25%

w/v Coomassie Brilliant Blue R-250 (in 10% v/v acetic acid and 20% v/v i-propanol solution) for 1 hour at room temperature rinsed and mounted. Images were collected by photographing consecutive non-overlapping fields.

2.5. Assessment of spreading and polarization of cells

Average cell area was used to determine the spreading of cells. Circularity index ($4\pi S/P^2$, where S is the cell area and P is the perimeter) was applied to define their polarization. A value of 1 represents a perfect circle, while a value close to 0 indicates an extremely elongated shape. For each experimental condition a total of 200 cells from three independent assays were analysed. Images of Coomassie-stained cells were photographed and analysed using *ImageJ* software. To define the boundaries of cells several commands were applied – *Threshold* (converts images to binary scale), *Close-* and *Fill Holes* (fill holes), *Remove Outliers* (reduces noise), *Watershed* (parts incorrectly merged objects). Cell selection was made by the *Wand (Tracing) Tool*. Spatial calibration was set towards an object micrometer and all numbers were calculated in μm.

2.6. Assessment of cell adhesion contacts

All adhesion sites in five representative cells from three independent experiments were used as a basis for generation of quantitative data sets. TIFF images were processed with *ImageJ* as follows: *Subtract background, Colour Balance, Clear outside, Merge channels*. The boundaries of cells were defined through the *Polygon selections Tool* and the cell area was calculated with *ROI Manager*. The total area of adhesion contacts per cell was separately calculated for red and green fluorescence. A manual threshold-based segmentation was used to create an adhesion contacts mask (*Threshold*). The adhesions were selected with *Wand tool* and *Create selection* and their total area calculated with *ROI Manager*. Selections were adjusted manually to eliminate aberrant signals as positive. Calibration was set towards an

object micrometer and all numbers were calculated in μm. Usually, FA and FbA lie in different planes of focus which demanded the merger of two or more images of GFP-tensin.

2.7. Statistical analysis

Statistical significance of multiple groups was determined by ANOVA and a Tukey-Kramer multiple comparisons analysis was used as a post hoc test. Calculations were performed using InStat software.

3. Results and discussion

3.1. Design of the biosensor

The concept of biosensors started with the creation of the so called analytical biosensors - devices comprised of biological and physicochemical component. The biological recognition element is usually an enzyme, nucleic acid, cell receptor, antibody, cell or tissue, linked to, or containing a signal transduction component converting the ligand-binding event into measurable signal, such as fluorescence, colorimetric, electrochemical, or magnetic response [13]. Typically these elements are limited to the detection of a single analyte.

The fluorescent-based biosensors usually relay on the shift in emission wavelength or interchange between on/off state of the fluorophore after detection of the analyte. Unlike this, the biosensor developed by us is based on constant signals, emitted by two fluorescently-tagged proteins localized at different cell sites - focal and fibrillar adhesions. As a proper choice we found the fluorochromes EGFP and mCherry as their emission wavelengths of 509 and 610 nm, green and red respectively, were easily distinguishable. For simultaneous identification of the two major adhesion types we utilized the specific cellular distribution of vinculin and tensin. Since both proteins are found in FA [8] these adhesions can be identified as places where mCherry and GFP signals overlap (GFP-positive/mCherry-positive). Moreover this double labelling allowed us to exclude the false-positive signal, coming from

the free cytoplasmic vinculin (GFP-negative/mCherry-positive). While most studies, investigating the adhesive properties of new materials keep their focus on FA formation only [2], we included the fibrillar adhesions as an additional important factor for assessing biocompatibility. Being an indicator of cell's activity to build up its own extracellular matrix [4, 5], well developed FbA could be regarded as a positive sign for integration of the new material into the host tissue. Because FbA contain no vinculin [11, 12], these adhesions could be identified as GFP-positive/mCherry-negative areas. To our knowledge, this is the first fluorescent biosensor where the readout is based on topology of the signals instead of changes in intensity or wavelength of fluorescent emission.

To create the biosensor a combination of pRKGFP-tensin/pmCherry-vinculin/pHA262 Puro A expression constructs was used for co-transfection of NIH/3T3 fibroblast cells carried out by electroporation. The presence of Neomycin resistance gene within pmCherry-vinculin vector and puromycin resistance plasmid pHA262 Puro A allowed to impose strong double antibiotic selection. The obtained antibiotic-resistant cells were subjected to cloning by limiting dilution. Sixty four clones were analysed for expression of tagged proteins by fluorescent microscopy. Several clones were regarded as acceptable variants and one - VT1.9 - exhibited the most satisfying intensity of both fluorescent signals and low signal to noise ratio. There, as expected, mCherry and GFP fluorescence were colocalized in the oval to elongated structures of focal adhesions, and only GFP-tensin, was detected in the threadlike fibrillar adhesions (Fig. 1A).

Further confirmation for the correct expression of the transfected constructs was obtained by immunoblotting. The molecular weight of vinculin is about 117 kDa [14]. While the parental NIH/3T3 cells demonstrated only one protein band matching the molecular weight of vinculin, in the VT1.9 sample an additional anti-vinculin positive band of about 147 kDa, representing mCherry-vinculin, was detected (Fig. 1B, vinculin). Similarly, only the selected

clone expressed a 250 kDa anti-GFP-positive protein corresponding to the predicted molecular mass of fluorescently tagged tensin (Fig. 1B, GFP).

The expression of fusion proteins may interfere with the normal function of their endogenous counterparts. Essential for our purposes were the conserved adhesion properties of the transfected VT1.9 cells. To assess their potential to adhere on substrates we carried out attachment tests on fibronectin coated coverslips. The results clearly demonstrated that the chimeric proteins had no impact on the adhesion capacity of biosensor cells (Fig. 1C). Based on these characteristics clone VT1.9 was selected for further development of the biosensor.

3.2. Standardization of the biosensor against natural ECM substrates

3.2.1. Determination of measurable parameters for assessment of cell-substrate interaction

We used mCherry-vinculin and GFP-tensin stably expressed in NIH/3T3 cells to detect a complex analyte that is the ability of specific substrate to support cell adhesion. The complexity of the analyte comes from the fact that cells respond differently to various physico-chemical properties of the adhesive surface. It has been repeatedly shown that wettability, roughness, topography and stiffness of the substrate influence cell behavior (for recent reviews see [7, 15, 16]). In addition, the presence of different chemical functional groups (CH_3, OH, COOH and NH_2) and ligand density have also been demonstrated to affect strongly cell adhesion [16, 17]. To analyze so many factors simultaneously we used the intrinsic ability of anchorage-dependent cells to process environmental cues and to respond accordingly. To assess substrate biocompatibility we identified four general and easily measurable parameters - cell spreading area, polarization, focal adhesion and fibrillar adhesion areas. These parameters are interrelated and each of them depicts important events in the process of establishing a contact between anchorage-dependent cells and the substrate. The events range from initial passive interactions, governed by physico-chemical properties of the cell surface and the substrate (net charge, viscosity of the ectoplasm etc.) [18, 19] to

more active latter occurring processes involving activation of integrin receptors; organization and engagement of actin cytoskeleton; activation of specific signalling pathways and building up of the multi-component adhesion sites [7, 20, 21]. Although the defined parameters do not provide specific information for the underlying events, they allow obtaining a general insight for adhesive properties of the substrate and offer a relatively simple way of estimating surface biocompatibility of new materials.

3.2.2. Measuring spreading and polarization of the biosensor on natural substrates

To standardize the biosensor behavior we used as substrates some of the major ECM components namely fibronectin, vitronectin, laminin-111, laminin-521 and collagen type I. The amounts of protein used for coating were determined by attachment assays as described by Humphries [22]. The following concentrations were used: 2.5 μg/cm^2 fibronectin, 2.5 μg/cm^2 vitronectin, 5 μg/cm^2 laminin-111, 2 μg/cm^2 laminin-521 and 5 μg/cm^2 collagen type I. Adhesion on untreated glass surface was also assayed.

To evaluate the behavior of biosensor on natural substrates, VT1.9 cells were plated sparse to avoid possible cell to cell contacts. In addition, the experiments were carried out in serum-free medium to prevent non-specific adsorption of serum-originating fibronectin and vitronectin. One hour after plating samples were fixed, stained and the mean value for cell spreading area (CSA) was measured. The most favorable spreading conditions were offered by fibronectin (CSA 1952±210 μm^2), followed by laminin-521 (CSA 1815±206 μm^2), laminin-111 (CSA 1208±370 μm^2) and vitronectin (CSA 908±71 μm^2) (Fig. 2A). As expected, most of the natural substrates induced better spreading than uncoated glass where CSA was around 500 μm^2 (556±60). The only exception was collagen I where CSA (422±21 μm^2) was even slightly decreased. Despite the fact that collagen I is produced by fibroblasts and is a major component of their native ECM, other studies have also documented limited spreading *in*

vitro [23]. A possible explanation of this result can be related to a high ligand density, used in our experiments. Gaudet *et al.* have shown that high coating density of collagen I turns into inhibitory factor for spreading of fibroblasts because the integrin receptors become saturated over a smaller distance [24]. Since we determined the coating concentration on the basis of cell attachment assay, 5 μg/cm^2 may exceed the optimal spreading coating density for collagen.

When steady radial spreading is completed and the cytoskeleton-generated contractile forces increase, the process of cell polarization begins. To determine the effect of different substrates on this process, VT1.9 cells were analyzed three hours after plating. Polarization was assessed on the basis of the circularity index (CI) where smaller values of the index indicate stronger polarization (Fig. 2B). The strongest polarization was registered for cells plated on fibronectin (CI 0.43±0.15) and laminin-111 (CI 0.43±0.19) followed by laminin-521 (CI 0.55±0.15). Again, the least effective but still better than uncoated glass (CI 0.7±0.13) were vitronectin (CI 0.65±0.15) and collagen I (CI 0.69±0.17). The acquisition of anterior-posterior polarity by cells is a complex process powered by Rho-mediated cell contractility [25]. The established activation of Rho by fibronectin and laminin-111 [26, 27] may explain the strongest polarization registered in our experiments.

3.2.3. Measuring of focal and fibrillar adhesions organized by the biosensor on natural substrates

The mCherry-tagged vinculin, expressed by biosensor cells, demonstrated well defined focal adhesion localization, but part of it was detected around cell nuclei in a free cytoplasmic form (Fig. 1A and 3A). Therefore only GFP-positive/mCherry-positive areas were used for FA determination, while areas with red signal only (Fig. 3A, black areas in adhesion outlines) were excluded. The largest mean values for focal adhesion area per cell (FAA) were measured

for laminin-521 (256±35 μm^2). As with the previous tests, fibronectin (FAA 231±30 μm^2) and laminin-111 (FAA 201±46 μm^2) performed better than collagen I (FAA 161±24 μm^2) and vitronectin (FAA 156±32 μm^2). The smallest focal adhesion area was measured for uncoated glass surface (FAA 119±24 μm^2) (Fig. 3B).

To assess the ability of different substrates to facilitate the organization of ECM we determined the mean values of the area, occupied by fibrillar adhesions. In view of the fact that GFP-tensin localized in both focal and fibrillar adhesions we calculated fibrillar adhesions area (FbAA) by subtracting the FAA from the area, defined by the green fluorescent signal for each studied cell. The results indicated that the capacity of different substrates to support formation of FbA decreased in the order Ln-521 (FbAA 208±71 μm^2)>CnI (FbAA 90±17 μm^2)>Fn (77±37 μm^2)>Ln-111 (FbAA 51±39 μm^2)>Vn (FbAA 47±24 μm^2)>glass (FbAA 41±16 μm^2) (Fig. 3C). Since fibrillar adhesions are formed by tensin-dependent α5β1 integrin translocation out of focal adhesions [4] substrates stimulating FA formation would be expected to promote the development of FbA. Our results confirmed this correlation for all studied substrates but collagen I. Although collagen I performed poorly in FA formation tests (Fig. 3B), it was the second best substrate for organization of FbA. A possible explanation may come from the established fact that collagen I and fibronectin bind and cooperate in the organization of extracellular matrix [28]. Moreover, certain collagen I conformations can promote fibronectin secretion by fibroblasts [29]. Since our experiments were implemented in the absence of serum, organization of fibronectin fibrils and the formation of FbA would solely depend on fibronectin, secreted by biosensor cells during overnight incubation. Thus, increased fibronectin secretion, stimulated by collagen I may account for the large FbAA, measured for this substrate.

Overall, determination of the values for spreading, polarization, focal adhesion area and fibrillar adhesion area for the studied natural substrates allowed us to outline the standard

behavior of biosensor cells and to build the "adhesion quality map" (graphs on Fig. 2 and 3B and C). Although in most of the assays fibronectin and the two laminins performed best, we did not find strict quantitative correlation between the four parameters. For example collagen I was the poorest substrate for spreading and polarization but it was the second best after Ln-521 in regard to organization of fibrillar adhesions (compare Fig. 2 and 3C). Similarly, while fibronectin promoted the strongest spreading and polarization (Fig. 2), it was less effective than Ln-521 which showed larger areas, occupied by FA and FbA (Fig. 3C). This lack of correlation most probably reflected the fact that each of the studied parameters represented different aspects of the cell adhesion process and confirmed that all four should be taken into account when a new and unknown material is characterized.

3.3. Application of the biosensor for biocompatibility assessment of PDMS-based substrates

Polydimethylsiloxane (PDMS) is widely used for fabrication of microdevices because of its advantages like biocompatibility, gas permeability, optical transparency and low manufacturing cost. However, the high protein adsorbtion and hydrophobicity of native PDMS [30] pose a significant obstacle for applications, requiring interactions with cells and tissues. Different modification techniques like changing chemical composition of PDMS, surface oxidization and coating with charged molecules have been applied in attempts to promote cell adhesion [31]. Potential improvement can be achieved by preparation of PDMS block polymers like poly(dimethylsiloxane-b-acrylic acid) (PDMS-PAA) and poly(dimethylsiloxane-b-vinyl pyrrolidone) (PDMS-PVP), where incorporated PAA and PVP enhance wettability and thus - tissue compatibility [32, 33]. To assess the adhesion properties of PDMS block polymers, biosensor cells were plated on PDMS-PAA and PDMS-PVP and the samples were prepared and analyzed as described for the natural substrates. Cells attached on both substrates, but spreading was more pronounced on PDMS-PAA (Fig. 4A). The

calculated mean CSA value for PDMS-PAA was about 70% higher (CSA 519±111 μm^2) than the one found for PDMS-PVP (CSA 302±8 μm^2) (Fig. 5A).

The inability of biosensor cells to spread on PDMS-PVP affected their polarization. While three hours after plating on PDMS-PAA, cells developed elongated morphology, PDMS-PVP-plated cells had predominantly circular shape (Fig. 4A, 3 h, insets). These observations were confirmed by measurement of the circularity index. Cells on PDMS-PAA had statistically significant ($p<0.001$) smaller CI (0.63±0.13) than the cells on PDMS-PVP (CI 0.73±0.12) (Fig. 5B).

To study the ability of PDMS-based substrates to support organization of FA and FbA the distribution of mCherry-vinculin and GFP-tensin was assayed after overnight incubation, but to get more information about the initial stages of adhesion, samples after 1 and 4 hours were also prepared. The results demonstrated that even after the first hour on PDMS-PAA, small dot-like focal adhesions, marked by co-localization of vinculin and tensin was possible to be detected. They were better developed after 4 hours and become morphologically identical to classical FA [3] after overnight incubation. Concomitantly, numerous and long fibrillar adhesions were detected after this prolonged incubation period (Fig. 4B). Unlike this, PDMS-PVP did not provide suitable conditions for organization of cell adhesions at early plating times. Vinculin and tensin remained largely disorganized and could be detected at adhesion sites only after incubation for overnight (Fig. 4B). Calculations of the adhesion areas supported the morphological observations. Both FAA (85±16 μm^2) and FbAA (34±18 μm^2) for cells, plated on PDMS-PAA were larger than the ones, measured for PDMS-PVP - FAA (33±11 μm^2) and FbAA (7±6 μm^2). Overall, a significant difference was observed between the two copolymers and PDMS-PAA attested itself as the polymer to offer more advantageous features than PDMS-PVP. This is most probably due to the incorporated COOH

groups which has been shown to promote formation of fibrillar adhesions and fibronectin fibrillogenesis [34].

To make a general evaluation of PDMS substrates biocompatibility the results for spreading, polarization, FAA and FbAA were plotted on the "adhesion quality map" (Fig. 5). This general comparison revealed that PDMS-PAA performed better than some of the natural substrates in terms of supporting spreading (CSA of PDMS-PAA>CSA of CnI) and polarization (CI of PDMS-PAA is almost equal of CI for Vn and CnI), and came close to them in promoting formation of fibrillar adhesions. Moreover, this comparison provided evidence that the weakest point of PDMS-PAA is the strength of cell adhesion, manifested trough insufficient FAA. It also suggested that, although PDMS-PAA has superior cell adhesion qualities over PDMS-PVP, further improvements like micro-patterning [35] or plasma surface modifications [36], directed at enhancing cell adhesion strength can bring PDMS-PAA even closer to the natural cell substrates.

4. Conclusions

The results, described in this study demonstrated the feasibility of establishing a more systematic approach in the process of surface evaluation of new biomimetic materials. The approach included a live-cell biosensor (an NIH/3T3 cell clone, stably expressing fluorescently-tagged marker adhesion proteins), a set of four measurable parameters (spreading, polarization, focal adhesion area and fibrillar adhesion area) and "adhesion quality map", consisting of the mean values of these parameters, obtained for five natural cell substrates (fibronectin, vitronectin, laminin-111, laminin-521 and collagen I). The use of the stable cell line and defined parameters guaranteed the reproducibility and comparability of the results, obtained from different experiments, and allowed direct comparison when the adhesive properties of new materials were tested. Moreover this approach permitted the

identification of the weakest parameter in the adhesion quality of the tested material which allowed identification of possible focused actions for biocompatibility improvements.

This approach can be developed further by including new types of natural substrates, or even three-dimensional substrates in the "adhesion quality map". By using this strategy, additional and more specialised live-cell biosensors can be developed. They can be targeted at testing new materials designed for defined purposes like endothelial biosensors for artificial blood vessels, biosensors based on bone cells for testing materials for artificial bone etc. Such approach may help speeding up the biocompatibility screening of the hundreds of new materials developed for the needs of regenerative medicine every year.

Acknowledgements

The authors are grateful to Dr. Kenneth M. Yamada (NIDCR, NIH, Bethesda, USA) for kindly providing the expression vectors; Dr. Ivan Keranov (Public Research Center Henri Tudor, Luxembourg) and Dr. Anelia Kostadinova (Institute of Biophysics and Biomedical Engineering, BASciences, Bulgaria) for kindly providing PDMS-PAA and PDMS-PVP.

Funding

This work was supported by grant D01-1261/07 from the National Science Fund, Bulgaria.

References

[1] S. Huang, D.E. Ingber, The structural and mechanical complexity of cell-growth control, Nat Cell Biol. 1 (1999) E131-E138.
[2] G.R. Owen, D.O. Meredith, I. ap Gwynn, R.G. Richards, Focal adhesion quantification - a new assay of material biocompatibility? Review, European cells & materials. 9 (2005) 85-96; discussion 85-96.
[3] R. Zaidel-Bar, M. Cohen, L. Addadi, B. Geiger, Hierarchical assembly of cell-matrix adhesion complexes, Biochemical Society transactions. 32 (2004) 416-420.

[4] R. Pankov, E. Cukierman, B.Z. Katz, K. Matsumoto, D.C. Lin, S. Lin, C. Hahn, K.M. Yamada, Integrin dynamics and matrix assembly: tensin-dependent translocation of α5β1 integrins promotes early fibronectin fibrillogenesis, J. Cell Biol. 148 (2000) 1075–1090.
[5] M. Vicente-Manzanares, F. Sanchez-Madrid, Cell polarization: a comparative cell biology and immunological view, Developmental immunology. 7 (2000) 51-65.
[6] B. Geiger, J.P. Spatz, A.D. Bershadsky, Environmental sensing through focal adhesions, Nat Rev Mol Cell Biol. 10 (2009) 21–33.
[7] S. Di Cio, J.E. Gautrot, Cell sensing of physical properties at the nanoscale: Mechanisms and control of cell adhesion and phenotype, Acta biomaterialia. 30 (2016) 26-48.
[8] R. Zaidel-Bar, S. Itzkovitz, A. Ma'ayan, R. Iyengar, B. Geiger, Functional atlas of the integrin adhesome, Nat. Cell Biol. 9 (2007) 858-867.
[9] E.R. Horton, J.D. Humphries, J. James, M.C. Jones, J.A. Askari, M.J. Humphries, The integrin adhesome network at a glance, J Cell Sci. 129 (2016) 4159-4163.
[10] E. Zamir, M. Katz, Y. Posen, N. Erez, K.M. Yamada, B.Z. Katz, S. Lin, D.C. Lin, A. Bershadsky, Z. Kam, B. Geiger, Dynamics and segregation of cell-matrix adhesions in cultured fibroblasts, Nature Cell Biol. 2 (2000) 191–196.
[11] A. Bershadsky, A. Chausovsky, E. Becker, A. Lyubimova, B. Geiger, Involvement of microtubules in the control of adhesion-dependent signal transduction, Curr Biol. 6 (1996) 1279-1289.
[12] E. Zamir, B.Z. Katz, S. Aota, K.M. Yamada, B. Geiger, Z. Kam, Molecular diversity of cell-matrix adhesions, J. Cell Sci. 112 (1999) 1655–1669.
[13] F.-G. Banica, Chemical Sensors and Biosensors: Fundamentals and Applications, John Wiley & Sons, Inc., 2012.
[14] G.J. Price, P. Jones, M.D. Davison, B. Patel, R. Bendori, B. Geiger, D.R. Critchley, Primary sequence and domain structure of chicken vinculin, The Biochemical journal. 259 (1989) 453-461.
[15] L. Bacakova, E. Filova, M. Parizek, T. Ruml, V. Svorcik, Modulation of cell adhesion, proliferation and differentiation on materials designed for body implants, Biotechnology advances. 29 (2011) 739-767.
[16] D. Denning, W.H. Roos, Elucidating the molecular mechanisms underlying cellular response to biophysical cues using synthetic biology approaches, Cell adhesion & migration. 10 (2016) 540-553.
[17] M. Mrksich, What can surface chemistry do for cell biology?, Current opinion in chemical biology. 6 (2002) 794-797.
[18] S.P. Carey, J.M. Charest, C.A. Reinhart-King, Forces During Cell Adhesion and Spreading: Implications for Cellular Homeostasis, in: A. Gefen (Ed.), Cellular and Biomolecular Mechanics and Mechanobiology, Springer Berlin Heidelberg, Berlin, Heidelberg, 2011, pp. 29-69.
[19] H. Wolfenson, T. Iskratsch, M.P. Sheetz, Early events in cell spreading as a model for quantitative analysis of biomechanical events, Biophys J. 107 (2014) 2508-2514.
[20] M. Cohen, D. Joester, B. Geiger, L. Addadi, Spatial and temporal sequence of events in cell adhesion: from molecular recognition to focal adhesion assembly, Chembiochem : a European journal of chemical biology. 5 (2004) 1393-1399.
[21] M. Prager-Khoutorsky, A. Lichtenstein, R. Krishnan, K. Rajendran, A. Mayo, Z. Kam, B. Geiger, A.D. Bershadsky, Fibroblast polarization is a matrix-rigidity-dependent process controlled by focal adhesion mechanosensing, Nat Cell Biol. 13 (2011) 1457-1465.
[22] M.J. Humphries, Cell-Substrate Adhesion Assays, in, Current Protocols in Cell Biology, John Wiley & Sons, Inc., 2001, pp. 9.1.1–9.1.11.

[23] L. Thorne, W. Davies, S.C. Brown, C.A. Rice-Evans, J.A. Lucy, Cell spreading on collagen that has been exposed to reactive aldehydes, Biochemical Society transactions. 20 (1992) 369S.
[24] C. Gaudet, W.A. Marganski, S. Kim, C.T. Brown, V. Gunderia, M. Dembo, J.Y. Wong, Influence of type I collagen surface density on fibroblast spreading, motility, and contractility, Biophys J. 85 (2003) 3329-3335.
[25] L. Kjoller, A. Hall, Signaling to Rho GTPases, Exp Cell Res. 253 (1999) 166-179.
[26] J.H. Park, J.M. Ryu, H.J. Han, Involvement of caveolin-1 in fibronectin-induced mouse embryonic stem cell proliferation: role of FAK, RhoA, PI3K/Akt, and ERK 1/2 pathways, Journal of cellular physiology. 226 (2011) 267-275.
[27] H.N. Suh, M.O. Kim, H.J. Han, Laminin-111 stimulates proliferation of mouse embryonic stem cells through a reduction of gap junctional intercellular communication via RhoA-mediated Cx43 phosphorylation and dissociation of Cx43/ZO-1/drebrin complex, Stem cells and development. 21 (2012) 2058-2070.
[28] B.J. Dzamba, H. Wu, R. Jaenisch, D.M. Peters, Fibronectin binding site in type I collagen regulates fibronectin fibril formation, J Cell Biol. 121 (1993) 1165-1172.
[29] N. Marin-Pareja, M. Cantini, C. Gonzalez-Garcia, E. Salvagni, M. Salmeron-Sanchez, M.P. Ginebra, Different Organization of Type I Collagen Immobilized on Silanized and Nonsilanized Titanium Surfaces Affects Fibroblast Adhesion and Fibronectin Secretion, ACS applied materials & interfaces. 7 (2015) 20667-20677.
[30] E. Berthier, E.W. Young, D. Beebe, Engineers are from PDMS-land, Biologists are from Polystyrenia, Lab on a chip. 12 (2012) 1224-1237.
[31] L. Wang, B. Sun, K.S. Ziemer, G.A. Barabino, R.L. Carrier, Chemical and physical modifications to poly(dimethylsiloxane) surfaces affect adhesion of Caco-2 cells, Journal of Biomedical Materials Research Part A. 93A (2010) 1260-1271.
[32] I.L. Keranov, M. Michel, A. Kostadinova, V. Toniazzo, D. Ruch, T. Vladkova, Poly(N-Vinyl Pyrrolidone-b-Dimethylsiloxane) Electrospun Nanofibers: Preparation, Characterization and Biological Response, OJBiphy. 3 (2013) 148-157.
[33] I. Keranov, M. Michel, A. Kostadinova, S. Miloshev, T. Vladkova, Well-defined nanoparticles from poly(N-vinyl pyrrolidone-b-dimethylsiloxane) prepared by conventional radical polymerization, IJEIT. 3 (2014) 18-29.
[34] N. Faucheux, R. Tzoneva, M.-D. Nagel, T. Groth, The dependence of fibrillar adhesions in human fibroblasts on substratum chemistry, Biomaterials. 27 (2006) 234-245.
[35] J. Hu, C. Hardy, C.M. Chen, S. Yang, A.S. Voloshin, Y. Liu, Enhanced cell adhesion and alignment on micro-wavy patterned surfaces, PLoS One. 9 (2014) e104502.
[36] J. Hauser, J. Zietlow, M. Koller, S.A. Esenwein, H. Halfmann, P. Awakowicz, H.U. Steinau, Enhanced cell adhesion to silicone implant material through plasma surface modification, Journal of materials science. Materials in medicine. 20 (2009) 2541-2548.

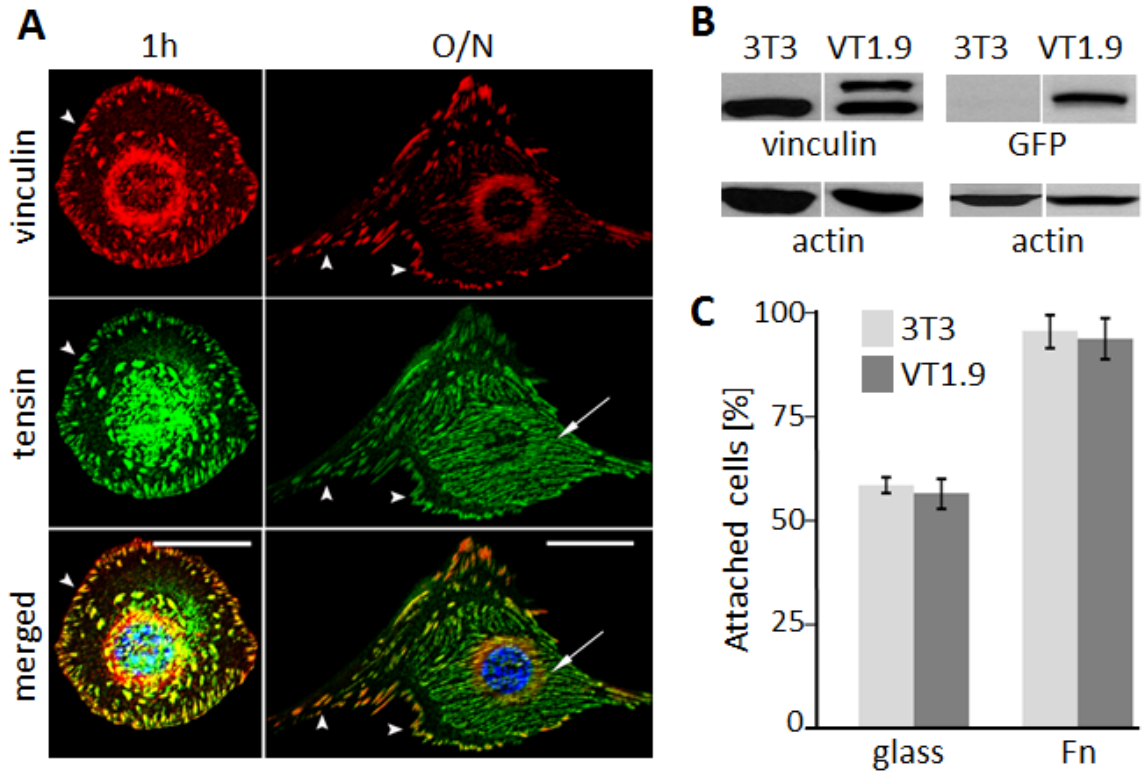

Fig. 1

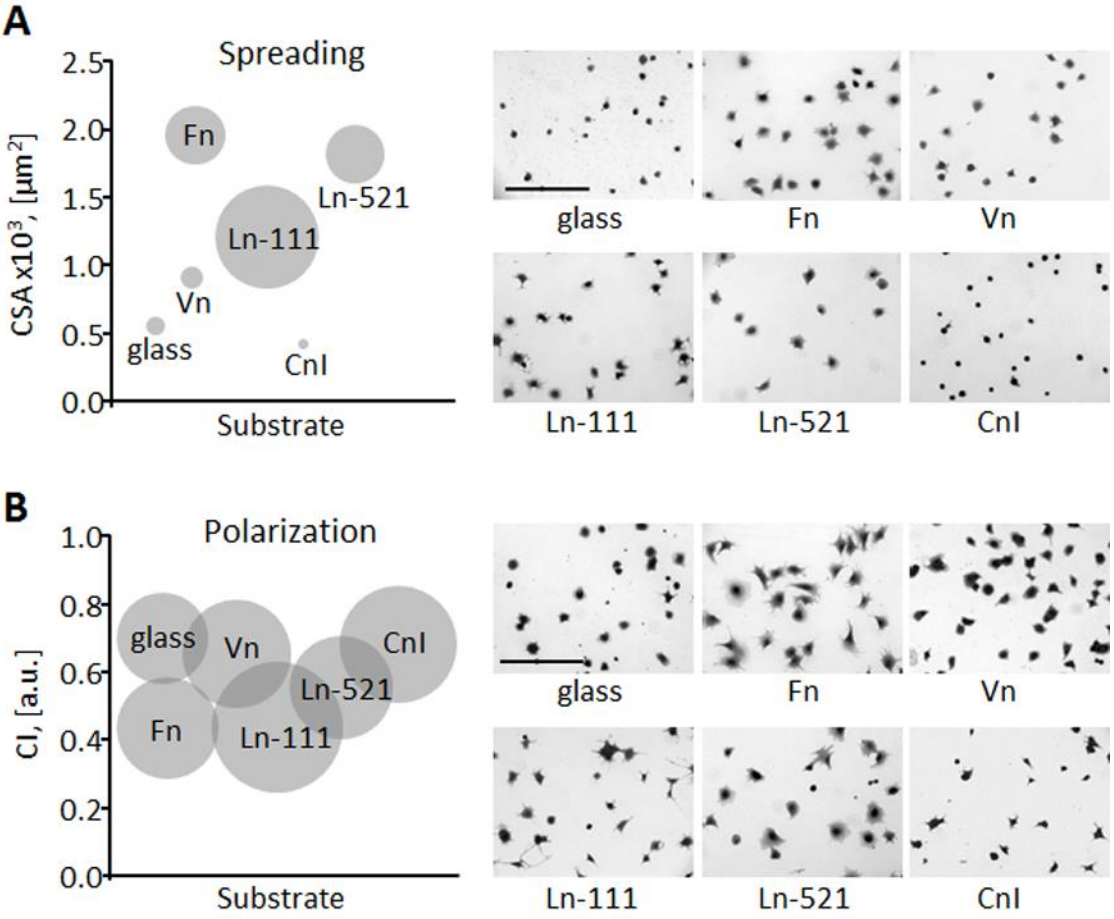

Fig. 2

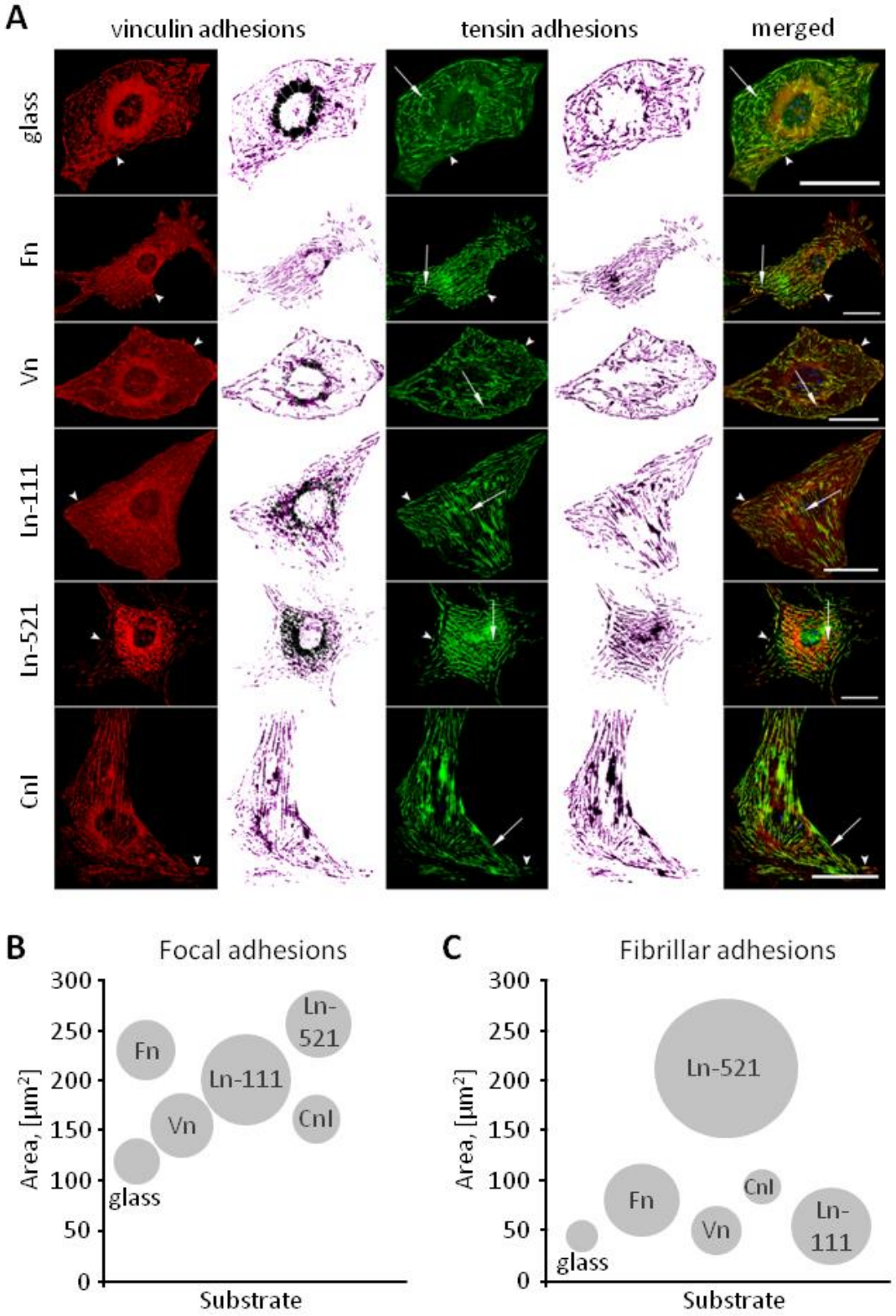

Fig. 3

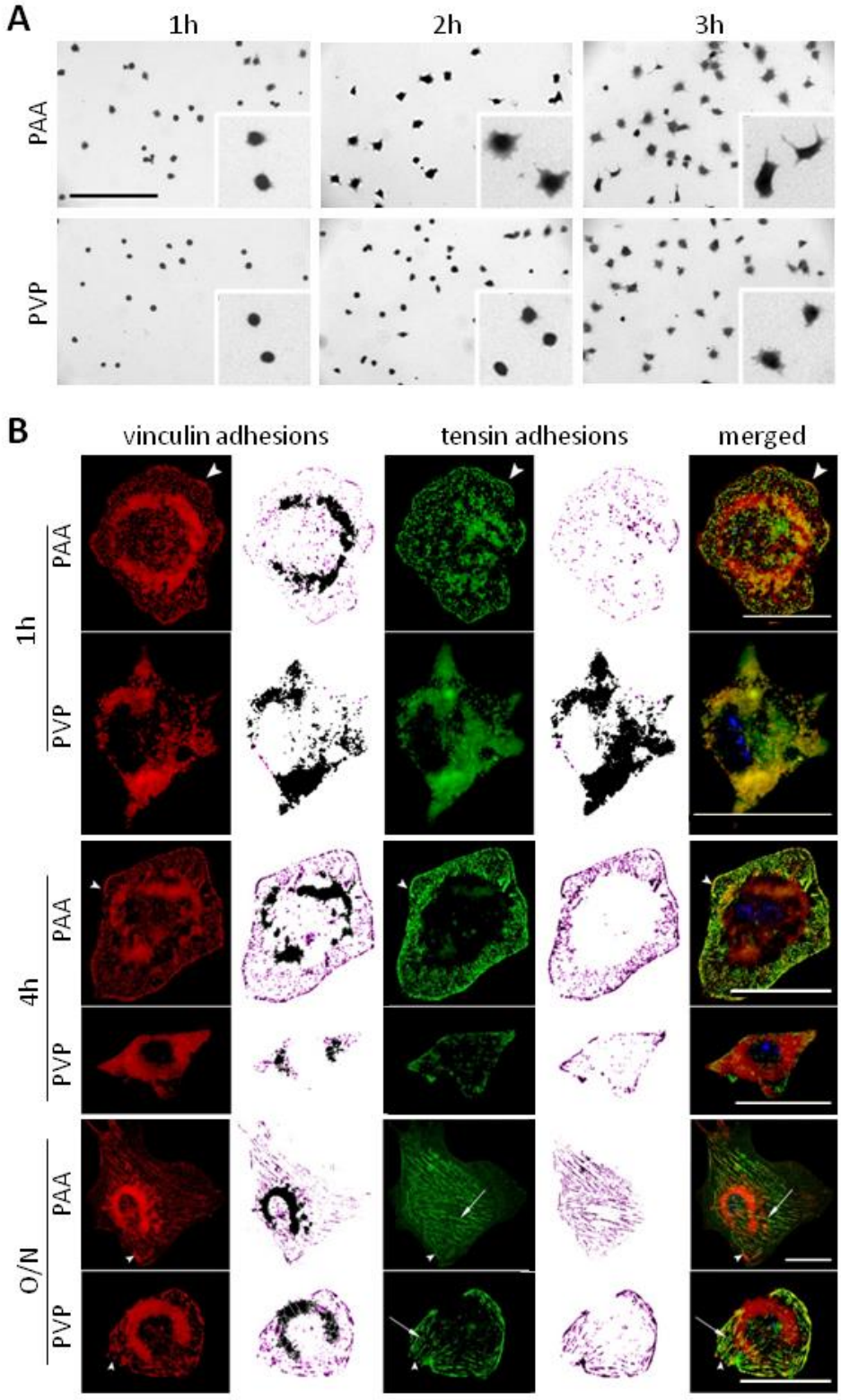
A
1h
2h
3h
PAA
PVP
B
vinculin adhesions
tensin adhesions
merged
1h
4h
O/N
PAA
PVP

Fig. 4

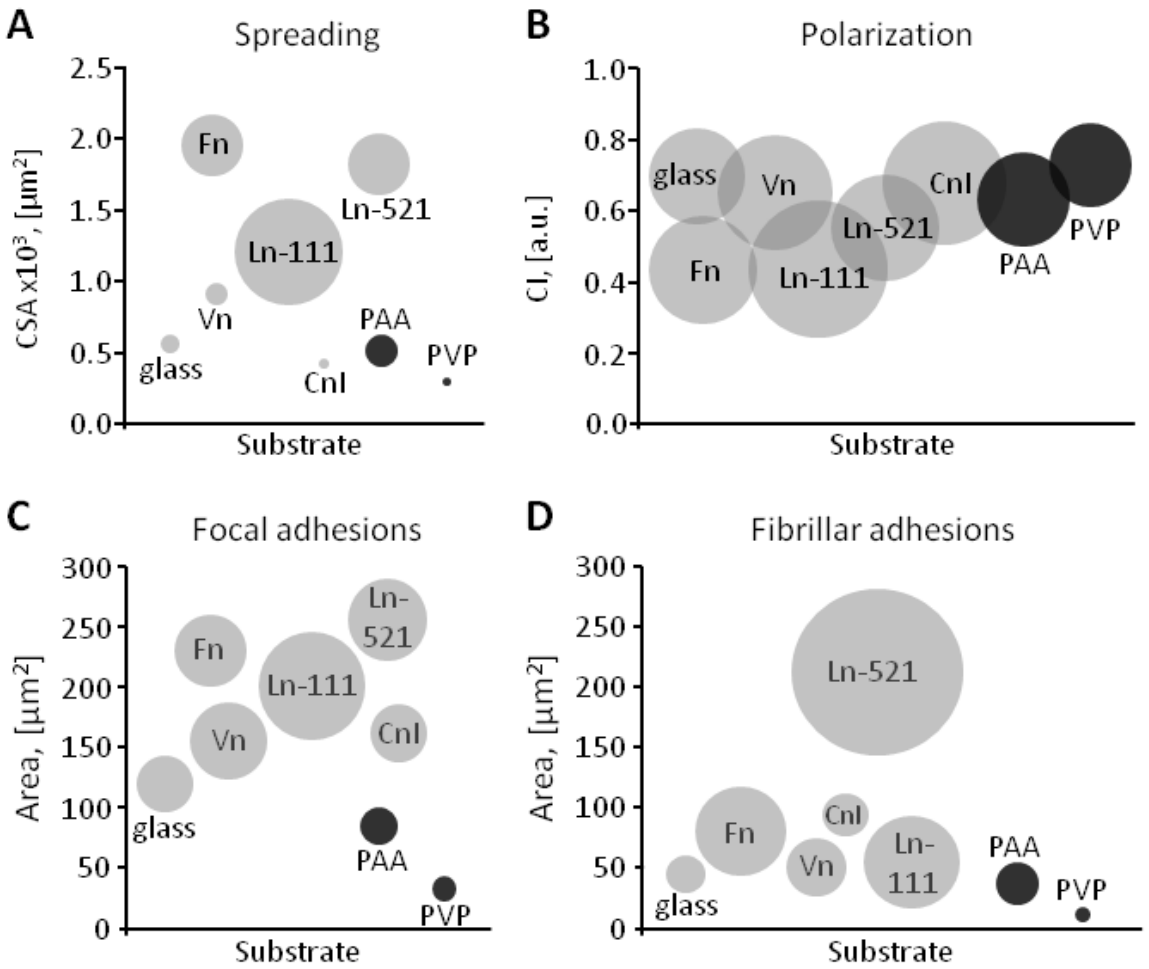

Fig. 5

Text to figures

Figure 1. Characterization of clone VT1.9. A) Distribution of fluorescent signals from transfected mCherry-vinculin (vinculin) and GFP-tensin (tensin) one hour (1 h) and overnight (O/N) after plating of cells on fibronectin. While GFP-tensin was detected in both FA (arrowheads) and FbA (arrows), mCherry-vinculin localized only in FA. Scale bar - 20 μm. B) Immunoblotting of total cell lysates from parental NIH/3T3 cells (3T3) and VT1.9 cells performed with anti-vinculin (vinculin) and anti-GFP (GFP) antibodies. Actin was used as control for protein loading. C) Adhesion potential of VT1.9 and NIH/3T3 fibroblasts. Cells were left to adhere on untreated (glass) and fibronectin (Fn) coated coverslips for one hour and the attached cells were counted. Error bars represent standard deviations. $p > 0.05$.

Figure 2. Spreading and polarization of biosensor cells on natural substrates. A) VT1.9 cells were plated for 1 hour on untreated (glass) or fibronectin (Fn); vitronectin (Vn); laminin-111 (Ln-111); laminin-521 (Ln-521) and collagen I (CnI) coated coverslips (right panel). The mean value of cell spreading area (CSA) is shown as a bubble graph where the radius of each bubble represents corresponding SD. B) For determination of cell polarization VT1.9 cells were plated for 3 hours on the same substrates as in "A". Representative images are shown on the right panel. The circularity index (CI), where a value of 1.0 stands for a perfect circle, while a value close to 0.0 indicates an extremely elongated shape, was used as an indicator of cell polarization. The mean value of CI for each substrate is presented on the left panel where the radius of the bubbles shows corresponding SD. Scale bar – 300 μm.

Figure 3. Focal and fibrillar adhesions, organized by biosensor cells on natural substrates. A) VT1.9 cells were plated for overnight on indicated substrates. Representative images, obtained from mCherry-vinculin (vinculin adhesions), GFP-tensin (tensin adhesions) and overlay of green and red channels (merged) are shown. Outlined adhesions, included in the calculations of the area are shown in purple, while the signals from non-localized protein are shown in black. Arrows indicate fibrillar adhesions; arrowheads - focal adhesions. Scale bar - 20 μm. The mean value of focal adhesion area (B) and fibrillar adhesion area (C) for each substrate are presented as bubble graphs. The radius of the bubbles shows corresponding SD.

Figure 4. Behavior of the biosensor cells on PDMS-based substrates. A) Cells plated for 1, 2 and 3 hours on PDMS-PAA (PAA) and PDMS-PVP (PVP) substrates were used for calculation of cell surface area and circularity index. Insets show typical cell morphology. Scale bar – 300 μm. (B) Representative images, obtained from mCherry-vinculin (vinculin adhesions), GFP-tensin (tensin adhesions) and overlay of green and red channels (merged), plated for 1, 4 hours and overnight (O/N) on substrates as in "A". Outlined focal and fibrillar adhesions, included in the calculations are shown in purple, while the signal from non-localized proteins are shown in black. Arrows indicate fibrillar adhesions; arrowheads - focal adhesions. Scale bar - 20 μm.

Figure 5. Assessment of surface biocompatibility of PDMS-based substrates with adhesion quality map. The mean values for: (A) cell surface area (CSA); (B) circularity index (CI); (C) focal adhesion area and (D) fibrillar adhesion area, calculated for biosensor cells plated on PDMS-PAA (PAA), PDMS-PVP (PVP), are presented as bubble graphs where the radius of the bubbles shows corresponding SD. For ease of comparison the corresponding values, obtained for the indicated natural substrates are also presented.

Highlights

- A live-cell fluorescent biosensor for general assessment of surface biocompatibility
- A standardizing "adhesion quality map", describing biosensor behavior on natural substrates
- Use of biosensor to demonstrate superior biocompatibility of PDMS-PAA over PDMS-PVP
- Use of biosensor to identify adhesive parameters of PDMS-PAA for further improvement